ADVANCED MATERIALS

Preparation of 7,16-(2′,3′-anthraceno)-7,16-dihydroheptacene ***(3)***: 90.0 g $AlCl_3$ was added in small portions at 0 °C and under Ar to a mechanically stirred solution of 19.05 g (75 mmol) triptycene and 36.70 g (225 mmol) phthalic anhydride in 1 L tetrachloroethylene. After complete addition, the cooling was removed and the mixture was heated to 100 °C for 20 h. The solution was cooled and poured into 750 mL of an ice/5 % aqueous HCl solution and stirred for one hour. The solids were then collected by vacuum filtration and dissolved in 10 % aqueous NaOH. The basic solution was filtered and acidified to pH 1. The resulting solids were filtered, washed with water, and dried in vacuo to give the tris-ketoacid derivative, **A**, as an off-white (pink to tan) solid, which is used without further purification.

A solution of **A** (from above) in 1 L concentrated sulfuric acid was heated to 100 °C for 17 h, cooled, and poured into 3 L crushed ice. The resulting solids were collected by filtration, washed with water, and dried under vacuum. The solids were then heated three times in 1.5 L boiling chloroform, and filtered. The organic solutions are combined and concentrated in vacuo. This solid was absorbed on to silica and subjected to flash chromatography with 1:1 chloroform/dichloromethane to give 6.31 g, 13 % yield (two steps), of the wholly symmetric **B** (R_f = 0.06) : ^{1}H NMR (300 MHz, $CDCl_3$): δ = 8.44 (s, ArH, 6H), 8.27 (dd, ArH, *J*= 6.0, 3.3 Hz, 6H), 7.78 (dd, ArH, *J* = 5.7 Hz, 3.5 Hz, 6H), 6.15 (s, CH, 2H); ^{13}C NMR (75 MHz, $CDCl_3$): δ = 182.7, 148.1, 134.4, 133.4, 132.6, 127.5, 123.2, 54.4; FT-IR(KBr): ν/cm^{-1}: 3056, 1673, 1617, 1594, 1322, 1288, 959, 720; HRMS (EI): Calcd. for $C_{44}H_{20}O_6$ (M+) 644.125989, found 644.1270 ± 0.0019. M.p. > 300 °C.

7.0 g Al and 1.0 g $HgCl_2$ were placed in a 500 mL Schlenk flask under Ar. 150 mL freshly distilled cyclohexanol (from Na) was added and the mixture was refluxed for one day in the dark. The solution was cooled below reflux temperature and 4.875 g (75.6 mmol) of **B** was added, followed by an additional 110 mL cyclohexanol, and the solution was heated back to reflux temperature for an additional day. The solution was then cooled, and the majority of the cyclohexanol was removed by distillation under vacuum to give a gummy green solid. A large volume of water was added to the solid and the solution was extracted with chloroform. The combined organic layers were washed with water and saturated NaCl (aq.), dried over $MgSO_4$, and concentrated in vacuo to give a suspension of solid in cyclohexanol. Addition of a ten-fold excess of methanol caused the precipitation of a crude solid, which was isolated by filtration. Column chromatography of the crude solid on neutral alumina with 2:1 hexane/dichloromethane gives a pale yellow solid, which can be recrystallized from hexane/dichloromethane to yield small needles of **3** (R_f = 0.44), 0.75 g (18 % yield). ^{1}H NMR (300 MHz, $CDCl_3$) δ = 8.30 (s, ArH, 6H), 8.05 (s, ArH, 6H), 7.93 (dd, ArH, *J*= 6.4, 3.3 Hz, 6H), 7.39 (dd, ArH, *J* = 6.6, 3.3 Hz , 6H), 5.83 (s, CH, 2H); ^{13}C NMR (75 MHz, $CDCl_3$): δ = 139.9, 131.8, 131.0, 128.2, 126.0, 125.2, 122.1, 53.3; UV ($CHCl_3$): λ_{max}/nm (logε): 281 (5.44), 329 (4.07), 345 (4.28), 363 (4.37), 381 (4.15); FT-IR(KBr): ν/cm^{-1}: 3038, 2998, 2949, 2925, 2852, 1677, 1426, 1296, 900, 738, 470; HRMS (EI): Calcd. for $C_{44}H_{26}$ (M+), 554.203451, found 554.2021 ± 0.0016. M.p. > 300 °C.

Received: September 1, 2000
Final version: December 12, 2000

[1] a) P. D. Beer, P. A. Gale, D. K. Smith, *Supramolecular Chemistry*, Oxford University Press, Oxford **1999**. b) J.-M. Lehn, *Supramolecular Chemistry*, VCH, Weinheim **1995**. c) F. Vögtle, *Supramolecular Chemistry*, Wiley, New York **1991**.
[2] X. Zhang, W. M. Nau, *Angew. Chem Int. Ed*. **2000**, *39*, 544.
[3] a) J.-S. Yang, T. M. Swager, *J. Am. Chem. Soc*. **1998**, *120*, 5321. b) J.-S. Yang, T. M. Swager, *J. Am. Chem. Soc*. **1998**, *120*, 11 864.
[4] F. G. Klärner, U. Burkert, M. Kamieth, R. Boese, J. Benet-Buchholz, *Chem. Eur. J*. **1999**, *5*, 1700.
[5] R. Rathore, J. K. Kochi, *J. Org. Chem*. **1998**, *63*, 8630.
[6] E. M. Veen, P. M. Postma, H. T. Jonkman, A. L. Spek, B. L. Feringa, *Chem. Commun*. **1999**, 1709.
[7] H. K. Patney, *Synthesis* **1991**, 694.
[8] a) J. Michl, E. W. Thulstrup, J. H. Eggers, *J. Phys. Chem*. **1970**, *74*, 3868. b) E. W. Thulstrup, J. Michl, J. H. Eggers, *J. Phys. Chem*. **1970**, *74*, 3878. c) J. Michl, E. W. Thulstrup, J. H. Eggers, *Ber. Bunsenges. Phys. Chem*. **1974**, *78*, 575. d) G. Gottarelli, B. Samori, R. D. Peacock, *J. Chem. Soc., Perkin Trans. 2* **1977**, 1208.
[9] a) J. Michl, E. W. Thulstrup, *Spectroscopy with Polarized Light*, VCH, Weinheim **1986**, pp. 129–221. b) J. G. Radziszewski, J. Michl, *J. Chem. Phys*. **1985**, *82*, 3527.
[10] J. W. H. Emsley, R. Hashim, G. R. Luckhurst, G. N. Shilstone, *Liq. Cryst*. **1986**, *1*, 437.
[11] H. Wedel, W. Haase, *Chem. Phys. Lett*. **1978**, *55*, 96.
[12] All calculations were performed with the Spartan program (Wavefunction, Inc.) on a Silicon Graphics O2 workstation. The geometries of **1–3** were optimized using semiempirical calculations (PM3). Distances were then measured as proton–proton centroid distances as shown in Figure 1.
[13] a) A. Ferrárini, G. J. Moro, P. L. Nordio, G. R. Luckhurst, *Mol. Phys*. **1992**, *77*, 1. b) E. E. Burnell, C. A. de Lange, *Chem. Rev*. **1998**, *98*, 2359. c) A. Ferrárini, P. L. Nordio, P. V. Shibaev, V. P. Shibaev, *Liq. Cryst*. **1998**, *24*, 219.
[14] I. Karacan, D. I. Bower, I. M. Ward, *Polymer* **1994**, *35*, 3411.
[15] a) H. Springer, J. Kussi, H.-J. Richter, G. Hinrichsen, *Colloid Polym. Sci*. **1981**, *259*, 911. b) H. Springer, R. Neuert, F. D. Müller, G. Hinrichsen, *Colloid Polym. Sci*. **1983**, *261*, 800.
[16] C. Weder, C. Sarwa, C. Bastiaansen, P. Smith, *Adv. Mater*. **1997**, *9*, 1035.

Fabrication of Nanometer-Scale Features by Controlled Isotropic Wet Chemical Etching**

By *J. Christopher Love*, *Kateri E. Paul*, and *George M. Whitesides**

This paper describes the application of a historically well-known phenomenon in lithography—undercutting by isotropic wet etching[1,2]—for the fabrication of nanostructures. We have combined conventional photolithography with simple isotropic wet etching to transfer the edges of a photoresist pattern into an underlying thin metal film by a two-step process. We etch isotropically, with controlled undercutting, through a thin metal film supported on a substrate of Si/SiO_2 or CaF_2. Subsequent deposition of a second thin metal film, followed by lift-off, defines trenches at the edges of each photoresist feature. This technique is an example of "edge lithography", a form of lithography in which the edges of the original pattern become the features of the final pattern. This technique generates structures with critical dimensions as small as 50 nm in a thin film of chromium or aluminum. The roughness of the edges produced is ~10–15 nm, and is limited theoretically to the grain size of the metal layer.

Convenient, inexpensive techniques for patterning features with nanometer-scale dimensions from the top down are an important component of nanoscience. In the short term, methods for producing nanometer-scale features that are already highly developed—DUV (deep ultraviolet), electron-beam (e-beam) writing, EUV (extreme ultraviolet), and X-ray photolithography[3,4]—will provide the basis for commercial production of microelectronic devices with features <100 nm. Fabrication of structures with nanometer-scale features appropriate for conducting exploratory research, for prototyping, and for fabricating simple devices are usually prohibitively expensive using advanced lithographic techniques; there is, therefore a place for simple methods that do not have the stability and reproducibility required for the fabrication of

[*] Prof. G. M. Whitesides, J. C. Love, K. E. Paul
Department of Chemistry and Chemical Biology
Harvard University
Cambridge, MA 02138 (USA)
E-mail: gwhitesides@gmwgroup.harvard.edu

[**] This research was supported by DARPA/AFRL/SPAWAR and used the MRSEC Shared Facilities supported by the NSF under Award No. DMR-9809363. JCL gratefully acknowledges the DoD for support in the form of a graduate fellowship. The authors thank Stephen Shepard and Yuanzhang Lu for their technical assistance.

  0935-9648/01/0804-0604 $ 17.50+.50/0

integrated circuits.[5] Controlled undercutting extends a general class of edge lithographies[6–11]—a part of the collection of soft-lithography techniques[12]—that utilize a two-step reduction process to transfer the edge of a pattern defined by conventional photolithography into features with critical dimensions below 100 nm on a substrate.

Isotropic wet etching is a simple and inexpensive technique for transferring a pattern defined by a physical mask, such as photoresist, into an underlying substrate. Typically, a metal film is oxidized selectively to a soluble (usually ionic) form by a strong acid or an oxidizing agent.[1,2] Polycrystalline metal films etch isotropically and yield structures with rounded sidewalls. The profile of the sidewall is sensitive to the temperature and composition of the etchant, and to the adhesion between the mask pattern and the metal film.[1,13] For high aspect-ratio structures, the variation in rates of etching makes it difficult to reproduce features exactly across wide areas. Undercutting by an isotropic etch in thick films is undesirable in general since the sidewalls of the etched structures are curved, and since it is difficult to define the width of the substrate that is exposed.

Typically, the use of wet etchants in industrial semiconductor processing is limited to cleaning and polishing substrates prior to patterning and to etching photoresist after exposure. Historically, overetching and undercutting photoresist patterns to decrease feature sizes is a well-known part of the lore of the semiconductor industry, but the techniques are not widely appreciated as an experimentally simple route to small structures for use in non-microelectronics applications. Isotropic wet etches are commonly used in micromachining to remove sacrificial layers and to release small micro- and nanostructures, such as beams and cantilevers, in microelectromechanical system (MEMS) devices.[14,15] Wet etches are also used to micromachine arrays of silicon field emission tips by etching pillars of silicon down to sharp points.[16–18]

Figure 1 summarizes the process for generating 50 nm scale trenches by controlled undercutting (see Experimental). As predicted from the isotropic etching profile, we find that the minimum size for an undercut feature that is etched completely down to the underlying substrate is dependent strongly on the film thickness. By comparison with the 50 nm features generated in 10 nm thick Cr, the minimum gap we could generate in a 35 nm thick Cr film is 100 ± 15 nm.

The roughness of the edge of the 50 nm gaps generated in the thin film of metal correlates with the size of the grains of the metal. For this reason, we used chromium and aluminum as the metal layer, since the grain size in films of these metals is ~15–25 nm. In contrast, the grain size of a gold film is ~50 nm when evaporated with an electron beam onto a room temperature substrate at 1.0 Å/s.

Gaps in thin films of chromium and aluminum are shown in Figure 2. Both straight and curved gaps are produced with the same linewidths. We find that the feature etched into the metal film accurately reproduces the contours of the photoresist pattern that was on top of the film prior to lift-off. The width of the gap can range from 50 nm to 200 nm depending on the etch time.

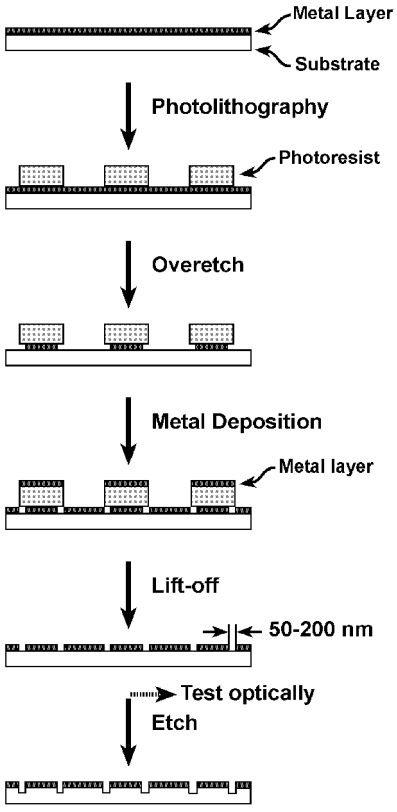

Fig. 1. Schematic illustration of the process used to generate nanometer-scale lines by controlled undercutting. A pattern is produced in the photoresist by photolithography or soft lithography. An isotropic etch is applied to the substrate beneath the photoresist. Shallow undercutting of the base layer, followed by evaporation into the exposed areas, and lift-off generates ~50–200 nm gaps in the thin film at the edges of the photoresist pattern. The pattern is then used as a physical mask for etching the substrate anisotropically or as an optical filter.

The metal film is sufficiently thick to serve as a good physical mask in a second etching process. Trenches with aspect ratios greater than those of the original metal film are obtained by reactive ion etching (RIE) of the underlying substrate. The scanning electron microscopy (SEM) images in Figure 3 show a cross section of a trench etched into Si ⟨100⟩ with SF_6/O_2. The metal masking layer can be removed later by wet etching to expose the underlying substrate.

One application for patterned thin films of metal is passive optical elements. Specifically, two-dimensional arrays of aperture elements with widths significantly smaller than the wavelength of the light used—frequency selective surfaces (FSS)—behave as strong bandpass filters.[19–22] Arrays of annular slots transmit light with a wavelength (λ_r) on the order of the average circumference of the rings in the array (Eqs. 1 and 2),[21]

$$\lambda_r \propto 2\pi R \text{ (for circular loops)} \quad (1)$$

$$\lambda_r \propto 4A \text{ (for square loops)} \quad (2)$$

where R is the radius of the loop and A is the length of the side of a square.

The width of the resonant peak in the transmission spectrum is controlled by the linewidth of the loops in the array. A

  0935-9648/01/0804-0605 $ 17.50+.50/0

ADVANCED MATERIALS

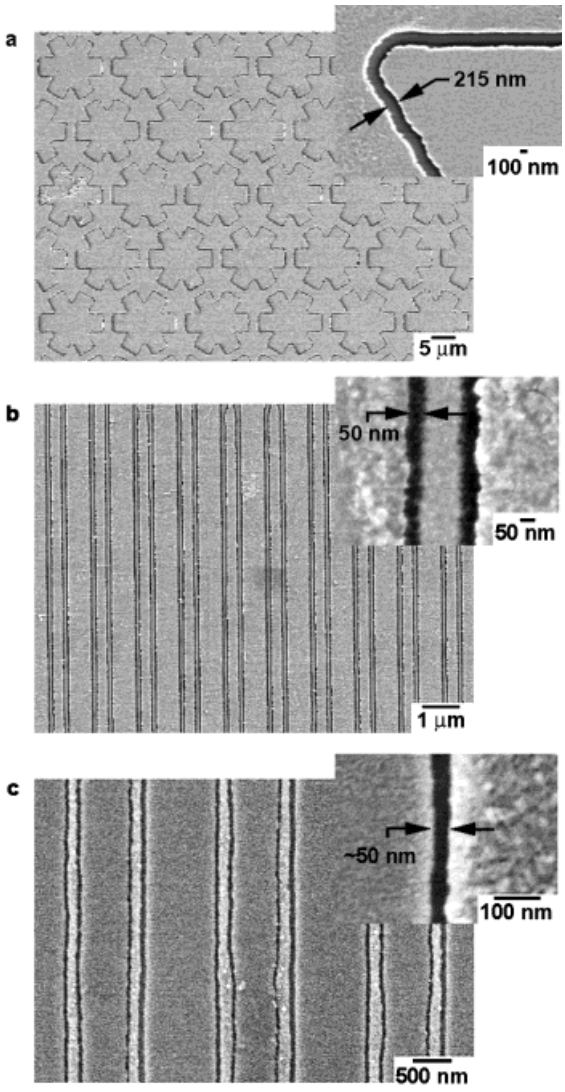

Fig. 2. SEM images of trenches formed in the thin chromium layer. The dark regions are the underlying Si/SiO_2 substrate. a) A 60 s etch resulted in a 215 nm trench outlining a star. The insert shows the trench following the contours of a corner of the star. b) An array of 50 nm trenches formed at the edges of 150 nm lines patterned by phase shift lithography and etched for 3 s. The insert shows a close-up detail of two trenches. Note that a trench forms at each edge of the original photoresist line. The images show the uniform width and edge contour replication of a trench generated in chromium by this technique. The roughness of the edges of the trench is ~25 nm, corresponding approximately to the grain size of the evaporated chromium film. c) A 7 s etch of a thin film of aluminum on a Si/SiO_2 substrate patterned by conformal phase shift lithography using a poly(dimethylsiloxane) (PDMS) mask having 1 μm lines spaced by 1 μm. The width of the gap shown in the insert is 50 ± 10 nm.

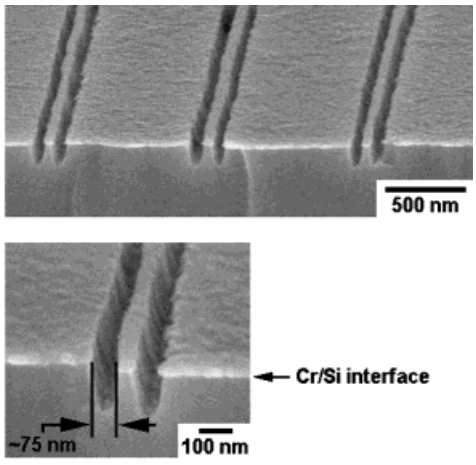

Fig. 3. SEM image of a cross section of linear trenches at the edges of a 100 nm line transferred into a Si <100> substrate. The trenches are 75 nm wide and 250 nm deep.

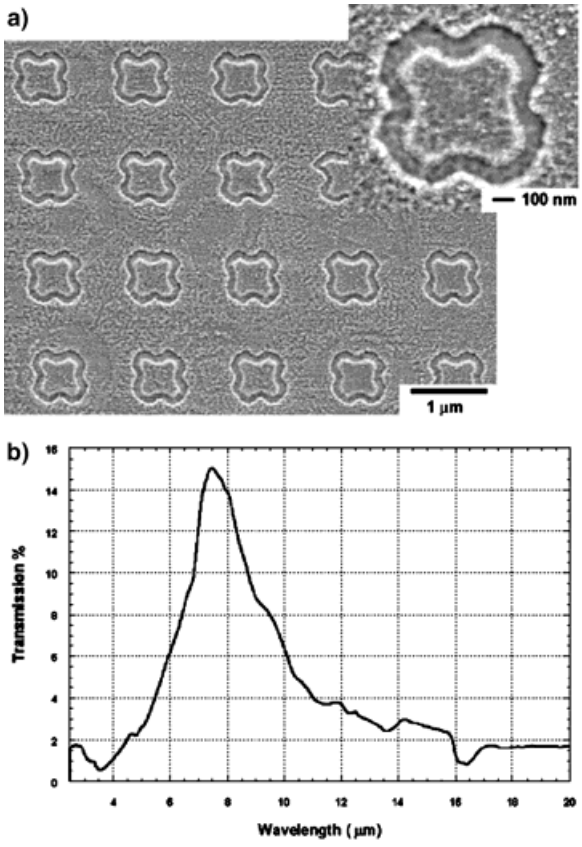

Fig. 4. a) An SEM image of an array of 800 nm square loops etched in a layer of aluminum with 100 nm trench widths on a substrate of optical grade Si/SiO_2. b) IR transmission spectrum measured through an array of loops in aluminum on optical grade silicon. The transmission peak at ~7.5 μm matches the theoretical predictions.

high quality factor (Q) for the transmission peak is attained by increasing the ratio of the average circumference of the ring to the width of the slot. A pattern of square loops with A ~ 800 nm etched into a 50 nm aluminum film on optical grade Si/SiO_2 had a resonant wavelength at ~7.5 μm in the infrared (IR) (Fig. 4). The thickness of the metal film was selected based on the skin depth of the metal to reflect all other wavelengths <40 μm.[23]

The key advantages of this undercutting technique are that: i) it uses any of a number of conventional or soft lithographic techniques to define the original pattern; ii) it utilizes a simple, inexpensive chemical process to generate uniform nanometer-scale linewidths in parallel across a large area (>4 cm^2); iii) it can be carried out in the open laboratory; iv) it controls the width of the features by the duration of etching and the

  0935-9648/01/0804-0606 $ 17.50+.50/0

etch solution chosen, rather than by the sizes of the features on a photomask; v) it is not limited by diffraction. The grain size of the thin metal film determines the resolution of the edges. The use of amorphous alloys or glasses may further reduce the critical dimensions generated by this technique.

In comparison to other forms of lithography—especially electron beam and scanning probe lithographies[24,25]—the key disadvantage of this technique is that it is the *edges* of the applied pattern that are transferred into the thin film; thus, the spacing between features (the pitch) is limited to the spacing of the original pattern. In addition, as with most isotropic etches, the resolution is also limited by heterogeneity in mass transport. This technique is useful for producing isolated features with narrow linewidths. Advanced photolithography could generate the original patterns of photoresist on the metal layer with smaller pitch than those demonstrated here, but are more complicated and less convenient.

In summary, this communication demonstrates that controlled undercutting is an inexpensive fabrication technique for transferring the edges of a patterned mask layer into an underlying, thin metal film. The edges are defined in the film using isotropic wet chemical etching followed by redeposition of a metal film and liftoff. The technique is useful for structures that do not require multiple-level registration and that are tolerant of defects; FSS are a good example. Etched 50 nm features across >4 cm^2 vary in width on average by 30 % (that is, slightly greater than the grain size of the metal). Possible applications include other subwavelength optics, nanofluidic systems, and simple, prototype electronic or optoelectronic devices.

Experimental

We deposited a thin metal film (10–50 nm Cr or Al) on clean Si/SiO_2 substrates by evaporation: electron-beam evaporation and thermal evaporation were used for chromium and for aluminum deposition, respectively. We primed the metal layer with hexamethyldisilazane (Microprime HP primer, ShinEtsu-MicroSi, Phoenix, AZ) and then applied a layer of photoresist (Shipley 1805, Shipley Corp., Marlborough, MA) on top of the metal layer by spin coating. The resist was patterned using standard contact-mode photolithography with broadband UV light (365–436 nm, Karl Suss MJB3 UV400) or by soft lithographic techniques, such as phase-shift lithography [10] and maskless lithography [11].

An isotropic wet etchant, specific to the metal film, transferred the photoresist pattern into the exposed areas of the film. We used commercially available wet etchants as delivered from Transene, Inc., Danvers, MA at the recommended temperatures for etching: Chromium Etch 1020 (cerium ammonium nitrate/nitric acid, 4 nm/s at 40 °C) and Aluminum Etchant Type A (phosphoric acid/nitric acid/acetic acid, 8 nm/s at 40 °C). We achieve the best control of etching by applying a stationary drop of the heated etchant onto a room-temperature substrate for a period of time determined by the thickness of the film and the desired width of the undercut region. We overetch the samples to produce shallow undercut regions in the metal layer at the edges of the photoresist pattern. Rinsing gently for 10 s with deionized water stopped the etching. Aluminum or chromium is redeposited by evaporation into the regions exposed on the substrate after etching. The photoresist shadows the undercut region during this evaporation. We then remove the photoresist layer to reveal the patterned surface.

For a 10 nm thick film of chromium, the typical etch time to produce undercut edges 50 nm in width is 3–4 s. Since the drop of etchant on the sample is not agitated, the rate is limited ultimately by diffusion. The diffusion-limited transport of fresh etchant to the undercut region decreases the rate as the initial reaction proceeds, and makes it possible to undercut regions 50 nm wide in 10 nm thick chromium. The experimental procedure is reproducible to ±15 nm, though the procedure must be calibrated by adjusting empirically the etching time for a given film thickness, composition, and etchant.

Received: September 4, 2000
Final version: December 13, 2000

[1] W. Kern, C. A. Deckert, in *Thin Film Processes* (Eds: J. L. Vossen, W. Kern), Academic, Boston, MA **1978**, p. 401.
[2] W. Kern, G. L. Schnable, in *The Chemistry of the Semiconductor Industry* (Eds: S. J. Moss, A. Ledwith), Kluwer, Dordrecht, The Netherlands **1987**, p. 225.
[3] P. Rai-Choudhury, *Handbook of Microlithography, Micromachining and Microfabrication* (Eds: A. J. Moses, J. Wood), IEEE Materials and Devices Series 12, Vol. 1, SPIE, Bellingham, WA **1997**.
[4] G. M. Wallraff, W. D. Hinsberg, *Chem. Rev.* **1999**, *99*, 1801.
[5] Y. Xia, J. A. Rogers, K. E. Paul, G. M. Whitesides, *Chem. Rev.* **1999**, *99*, 1822.
[6] J. A. Rogers, O. J. A. Schueller, C. Marzolin, G. M. Whitesides, *Appl. Opt.* **1997**, *36*, 5792.
[7] J. A. Rogers, K. E. Paul, R. J. Jackman, G. M. Whitesides, *J. Vac. Sci. Technol. B* **1998**, *26*, 59.
[8] J. Aizenberg, A. J. Black, G. M. Whitesides, *Nature* **1998**, *394*, 868.
[9] A. J. Black, K. E. Paul, J. Aizenberg, G. M. Whitesides, *J. Am. Chem. Soc.* **1999**, *121*, 8356.
[10] J. A. Rogers, K. E. Paul, R. J. Jackman, G. M. Whitesides, *Appl. Phys. Lett.* **1997**, *70*, 2658.
[11] K. E. Paul, T. L. Breen, J. Aizenberg, G. M. Whitesides, *Appl. Phys. Lett.* **1998**, *73*, 2893.
[12] Y. Xia, G. M. Whitesides, *Angew. Chem. Int. Ed.* **1998**, *37*, 550.
[13] R. Germann, in *Nanofabrication and Biosystems* (Eds: H. C. Hoch, L. W. Jelinski, H. G. Craighead), Cambridge University Press, Cambridge **1996**, p. 18.
[14] R. E. Oosterbroek, J. W. Berenschot, S. Schlautmann, G. J. M. Krijnen, T. S. J. Lammerink, M. C. Elwenspoek, A. v. d. Berg, *J. Micromech. Microeng.* **1999**, *9*, 194.
[15] H. Ohji, P. J. French, *Sens. Actuators* **1999**, *74*, 109.
[16] C. C. Umbach, B. W. Weselak, J. M. Blakely, Q. Shen, *J. Vac. Sci. Technol. B* **1996**, *14*, 3420.
[17] J. T. Trujillo, C. E. Hunt, *Semicond. Sci. Technol.* **1991**, *6*, 223.
[18] D. W. Kim, S. H. Lym, M. Y. Jung, H. T. Jeon, S. S. Choi, *Microelectron. Eng.* **1999**, *46*, 423.
[19] D. M. Byrne, A. J. Brouns, F. C. Case, R. C. Tiberio, B. L. Whitehead, E. D. Wolf, *J. Vac. Sci. Technol. B* **1984**, *3*, 268.
[20] K. J. Kogler, R. G. Pastor, *Appl. Opt.* **1988**, *27*, 18.
[21] P. A. Krug, D. H. Dawes, R. C. McPhedran, W. Wright, J. C. Macfarlane, L. B. Whitborn, *Opt. Lett.* **1989**, *14*, 931.
[22] C. M. Rhoads, E. K. Damon, B. A. Munk, *Appl. Opt.* **1982**, *21*, 2814.
[23] C. Kittel, *Introduction to Solid State Physics*, Wiley, New York **1976**.
[24] S. Hong, C. A. Mirkin, *Science* **2000**, *288*, 1808.
[25] P. Vettiger, M. Despont, U. Dreschler, U. Durig, W. Haberle, M. I. Lutwyche, H. E. Rothuizen, R. Stutz, R. Widmer, G. K. Binnig, *IBM J. Res. Dev.* **2000**, *44*, 323.

  0935-9648/01/0804-0607 $ 17.50+.50/0